Facile synthesis of SnS nanoparticles and SnS-rGO nanocomposites and its characteristics properties for multifunction application

A DISSERTAION REPORT

SUBMITTED IN PARTIAL FULFILLMENT OF THE REQUIREMENT FOR THE AWARD OF THE DEGREE OF

MASTER OF SCIENCE
IN
PHYSICS

Submitted By: -

HARDIK

(2k21/MSCPHY/16)

MSc Physics, 2nd year

Under the supervision of

Prof. Nitin Kumar Puri

DEPARTMENT OF APPLIED PHYSICS
DELHI TECHNOLOGICAL UNIVERSITY
(Formerly Delhi College of Engineering)
Bawana Road, Delhi-110042

May, 2023

DEPARTMENT OF APPLIED PHYSICS

DELHI TECHNOLOGICAL UNIVERSITY

(Formerly Delhi College of Engineering)

Bawana road, Delhi-110042

CANDIDATE'S DECLARATION

I, **Hardik (2K21/MSCPHY/16)** students of M.sc physics, hereby declare that the project dissertation titled "**Facile synthesis of SnS-rGO nanocomposite and it's characteristics properties for multifunction application.**" which is submitted to the **Department of Applied Physics, Delhi Technological University, Delhi** in partial fulfilment of the requirement for the award of the degree of Master in Science is original and not copied from any source without proper citation. This work has not previously formed the basis for the award of any Degree, Diploma Associateship, Fellowship, or other similar title or recognition.

Place: New Delhi

Date: 31/05/2023

HARDIK

DEPARTMENT OF APPLIED PHYSICS
DELHI TECHNOLOGICAL UNIVERSITY
(Formerly Delhi College of Engineering)
Bawana road, Delhi-110042

SUPERVISOR CERTIFICATE

I, hereby certify that the project dissertation titled "**Facile synthesis of SnS-rGO nanocomposite and it's characteristics properties for multifunction application.**", which is submitted by **Hardik (2K21/MSCPHY/16)** to the **Department of Applied Physics, Delhi Technological University** in partial fulfillment of the requirement for the award of grades of semester IV in Applied Physics is a record of the project work carried out by the student under my supervision. This work has not been submitted partially or completely during any degree or diploma to this university or anywhere else, to the best of my knowledge.
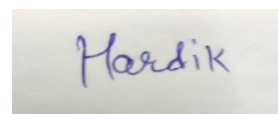
Place: New Delhi

Date: 31/05/23

Prof. Nitin Kumar Puri

DEPARTMENT OF APPLIED PHYSICS

Delhi technological University

<u>ACKNOWLEDGEMENT</u>

Abstract

Nanoparticles (NPs) have piqued the interest of researchers since their discovery due to their distinguishable properties and vast variety of uses. Various synthesis methods have been used to create semiconductor nanoparticles throughout the last few decades. And have piqued the curiosity of researchers due to their unusual features. In this work, we attempted to synthesize SnS NPs and SnS-rGO NCs using the hydrothermal technique. Ethylene glycol is used as a solvent, and thiourea is used as a sulfur source. Different approaches were used to characterize the synthesized SnS NPs and SnS-rGO NCs. The optical characteristics of synthesized materials are studied using UV-vis and photoluminescence (PL) spectroscopy. The FESEM technique is used to investigate material morphology. The elemental component has been examined using the EDS technique. The XRD pattern is used to investigate crystallinity and phase orientation. The synthesized SnS NPs and SnS-rGO NCs are in the orthorhombic phase, according to XRD analysis, and the crystallite size was determined using the Deby-Sheerer equation. The FTIR approach was utilized to confirm the presence of various functional groups in SnS NPs and SnS-rGO NCs synthesized.

Table of content

List of Figures

List of table

Table Number	Caption
4.1	hkl and d spacing value for SnS NPs and SnS-rGO NCs.
4.2	Calculated crystallite size using Scherrer equation and WH plot and strain.
4.3	Direct and indirect bandgap values of SnS NPs and SnS-rGO NCs.

List of Symbols and Abbrivations

Symbol/ Index	Meaning/ Abbrevation
SnS	Tin (II) Sulfide
rGO	Reduced Graphene Oxide
NPs	Nanoparticles
NCs	Nanocomposites
SA:V	Surface Area to Volume Ration
QCE	Quantum Confinement Effect
PVDF	Polyvinylidene Fluoride
XRD	X-Ray Diffraction
UV	Ultraviolet
UV-Vis	Ultraviolet-Visible
PL	Photoluminescence
FTIR	Fourier-Transform Infrared
FESEM	Field Emission Scanning Electron Microscopy
EDX	Energy Dispersive X-ray Spectroscopy

Chapter 1

Introduction

Nanoparticles (NPs) and nanocomposites (NCs) are new types of nanomaterials that have gained a lot of interest in the past few years. The term nanoparticle refers to a particle whose at least one of its three dimensions is in the nanoscale (1–100 nm) range. They are made of a few hundreds of atoms, likely 100–1000 atoms.

If we delve into the history of the nanoparticles, French researchers have discovered that 2000 years ago, Egyptians, Greeks, and Romans used sulfide nanocrystals with a diameter of 5 nm to dye their hair. Additionally, in the Middle Ages, around 1000 years ago, mediaeval artists used different sizes of gold nanoparticles on stained glass windows to produce different colours. On December 25, 1959, Richard Feynman, known as the father of nanotechnology, gave the lecture "There's a Plenty of Room at the Bottom: An Invitation to Enter a New Field of Physics" at the annual American physics society meeting at Caltech. He laid the groundwork for the concept of nanotechnology by giving the idea of understanding and manipulating materials and devices at the nanoscale level [1]. Which sparked interest and curiosity among the fellow scientists, engineers, and researchers. In 1974, the term "nanotechnology" came into existence, coined by the Japanese scientist Norio Taniguchi. In 1981, the scanning tunnelling microscope (STM) was discovered by IBM researchers [2]. The STM instrument has revolutionised the field of nanotechnology as it is capable of imaging the surface at the atomic scale. Its ability to visualise matter at such a fine resolution has greatly contributed to our understanding of nanoscale phenomena. In 1985, scientists at Rice University in the United States and the University of Sussex in the United Kingdom identified a new molecule composed of 60 carbon atoms arranged in a unique structure resembling a soccer ball, which they named C60 [3, 4]. This molecule, usually referred to as "buckyball" due to its resemblance to the geodesic domes designed, is known as a fullerene. Which is the class of carbon-based molecules that are composed entirely of carbon atoms in a close-cage structure. The discovery of C60 opened up a new field of research and sparked immense interest in the study of fullerene chemistry and its potential. In 1991, a Japanese physicist and inventor, Sumio Iijma, discovered carbon nanotubes (CNTs) with the help of an electron microscope [5]. The discovery of CNTs led to extensive research efforts to

understand their properties, synthesis methods, and potential applications. The CNT exploration has revealed several forms of CNTs, such as multi-walled nanotubes (MWCNTs) and single-walled nanotubes (SWCNTs)., each with their own characteristic properties. In 1999, Robert A. Freitas Jr. wrote the first book on nanomedicine, "Nanomedicine". The publication of "Nanomedicine" further inspires research, innovation, and collaboration in the field, leading to advancements in targeted drug delivery systems, biosensors, and other nanotechnology-enabled medical technologies. Which contributes to the growth of a new distinct field of nanobiotechnology. Currently, nano-related materials (nanoparticles, nanocapsules, nanotubes, nanocomposites, etc.) are becoming a rapidly growing technology, also referred to as nanotechnology.

Nanomaterials have shown unique and great properties over bulk materials, which arise due to their nanoscale dimensions and the influence of quantum and surface effects. Because of that, they have gained so much attention in recent years. Nowadays, nanomaterials have applications in various sectors, including electronics and optics, energy, medicine and healthcare, environmental remediation, aerospace defence, automotive, etc. The reason why we are highly interested in nanoparticles is because of their light weight, ability to access small spaces, cost-effectiveness, more energy efficient, and different properties for very small structures. There are two main approaches to making nanoparticles. One is a bottom-up approach, which includes chemical precipitation reactions, sol-gel synthesis, hydrothermal synthesis, etc., and the other is a top-down approach, which includes techniques like ball milling, lithography, etc.

1.1 Overview of the thesis

In this thesis, we have arranged our work into chapters and parts. This provides you with a fundamental overview of nanomaterials, their characteristics, applications, and synthesis. In Chapter 1, we reviewed the history of nanoparticles, their evolution, and some of their pros and cons. In Chapter 2, we reviewed the variables that influence bulk material characteristics at the nanoscale, various synthesis methods, and applications. In Chapter 3, we covered the approach used to synthesize the SnS NPs and SnS-rGO NCs. In Chapter 4, we described the many characterization approaches we used to explore the various characteristics of SnS NPs and SnS-rGO NCs.

Chapter 2

2.1. Factors responsible for enhancing and changing the properties of materials at nanoscale.

Fig.2.1 show the factors that are responsible for enhancing and changing the properties of materials when we go to the nanoscale levels. Which further discussed briefly.
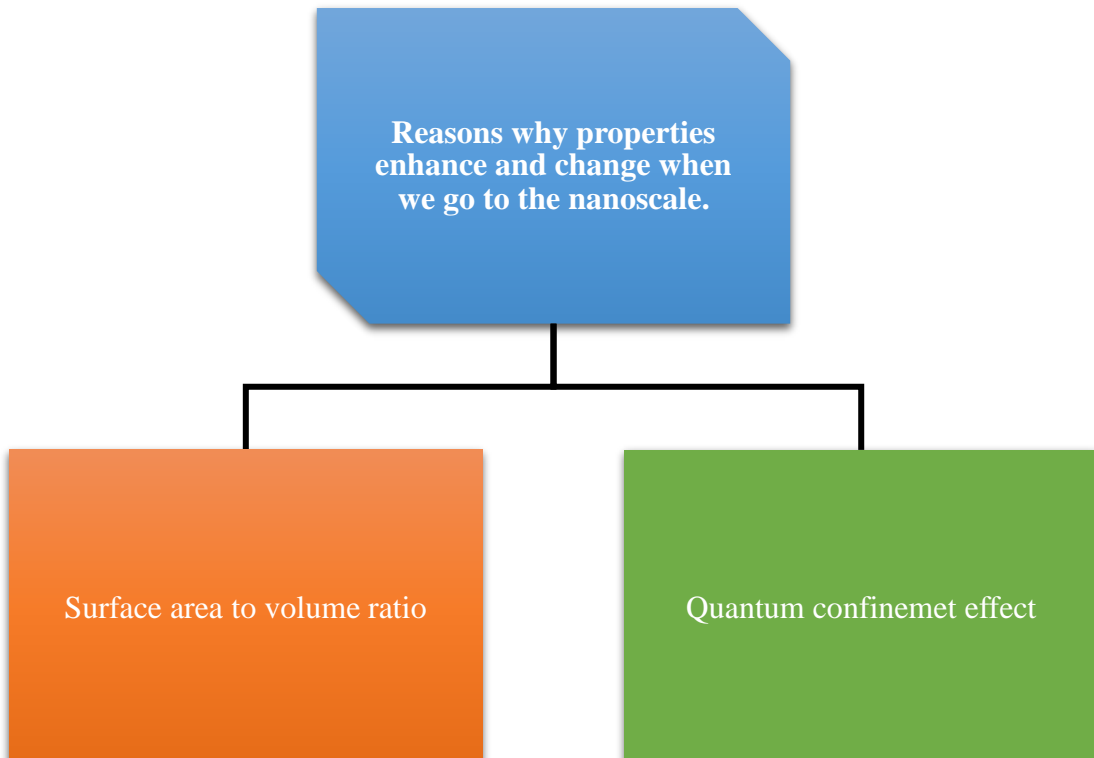
Fig2.1 Reasons why properties of the materials enhance and change at nano scale.

2.2 Surface area to volume ratio (SA: V)

It's a measure of the amount of surface area per unit volume of a three-dimensional material or object. "SA: V" can be obtained by dividing the object's surface area by its volume.

The "SA: V" is important because it influences the behavior and properties of materials at the nanoscale, and in the case of nanomaterials, the "SA: V" increases significantly. Because of that, nanomaterials exhibit unique properties and enhance reactivity as compared to bulk materials. fig.2.2 shows the properties that enhance or change due to the surface area to the volume ration.

```
Properties enhance or change due to the
surface area to the volume ratio
├── Reactivity
├── Surface energy
├── Mechanical properties
├── Optical properties
├── Absorption capacity
├── Catalytic activity
├── Electrical conductivity
└── Surface plasmon resonance
```

fig.2.2 properties enhance or change due to the surface area to the volume ratio.

2.3 Quantum confinement effect (QCE)

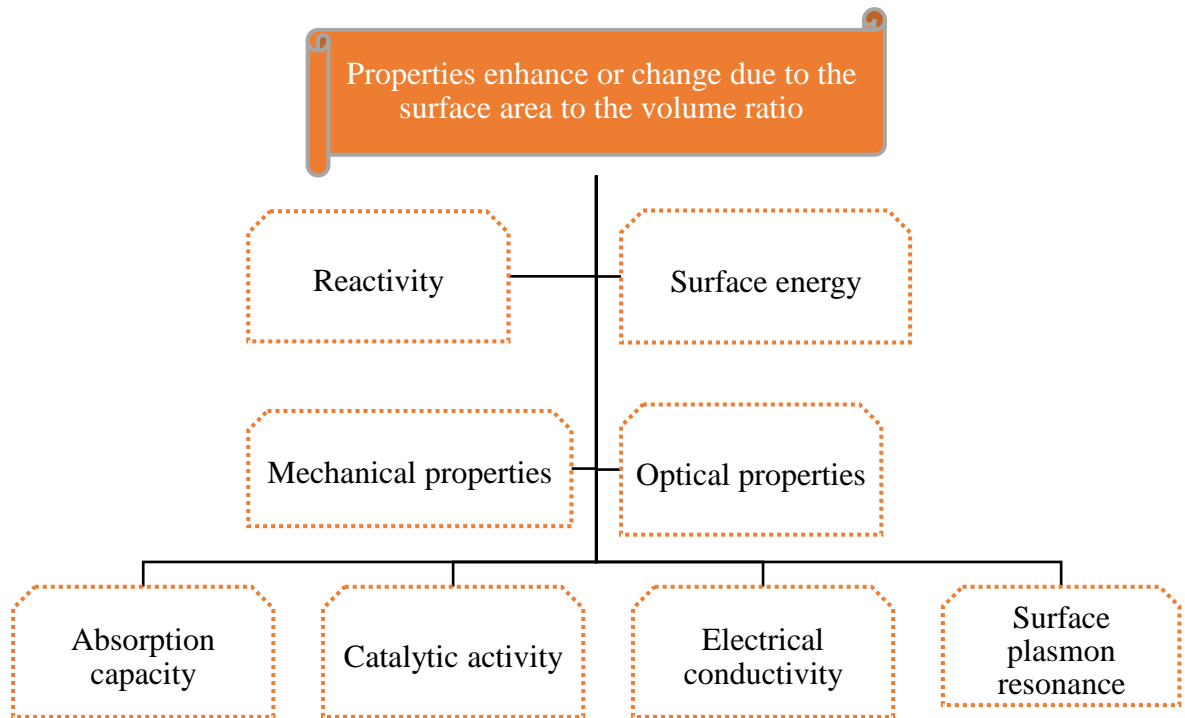The quantum confinement effect (QCE) refers to the phenomena observed in materials at the nanoscale. These phenomena occur when materials are confined to nanoscale dimensions, causing the energy level to become discrete (energy values are distinct and separated rather than continuous and varying smoothly) and quantized (energy values can only exist at certain levels or energy is restricted to specific values) due to the confinement of electron motion within a limited space. fig.2.3 shows the properties that enhance or change due to the QCE.

QCE can manifest in 0D, 1D, and 2D nanostructures. fig.2.4. show illustrative diagram of quantum confinement in all 0D, 1D. and 2D.

- In zero-dimension nanostructures, such as quantum dots, electronic states are confined in all three dimensions.
- In one-dimensional nanostructures, such as quantum wire (nanowires or nanotubes), the electronic states are confined to two dimensions. Means electrons can easily move in one direction.

4

- In two-dimensional nanostructures, such as quantum well (thin films or graphene), the electronic states are confined to one dimension. Means electrons can easily move in two directions [6].

Properties enhance or change due to the qunatum confinement effect

Bandgap tuning

Size dependent optical properties

Mechanical properties

Quantum confinement of charge carriers

Enhance photocatalytic activity

Size dependent magnetic properties

Enhance thermoelectric properties
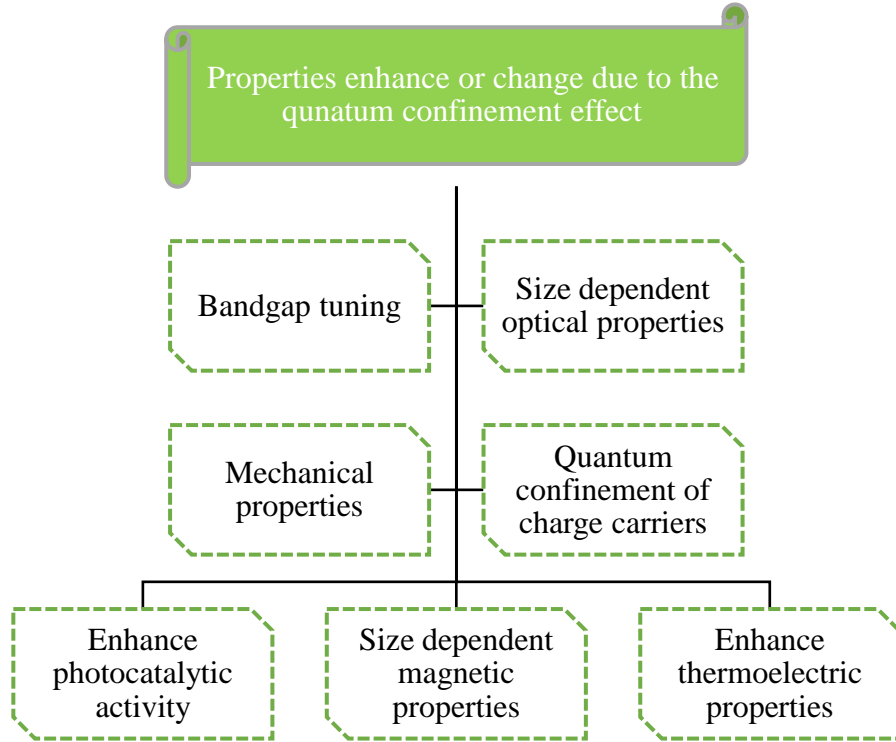
Fig 2.3 Properties enhance or change due to quantum confinement effect.

Quantum dot: motion confined in all directions

Quantum wires: motion confined in two directions

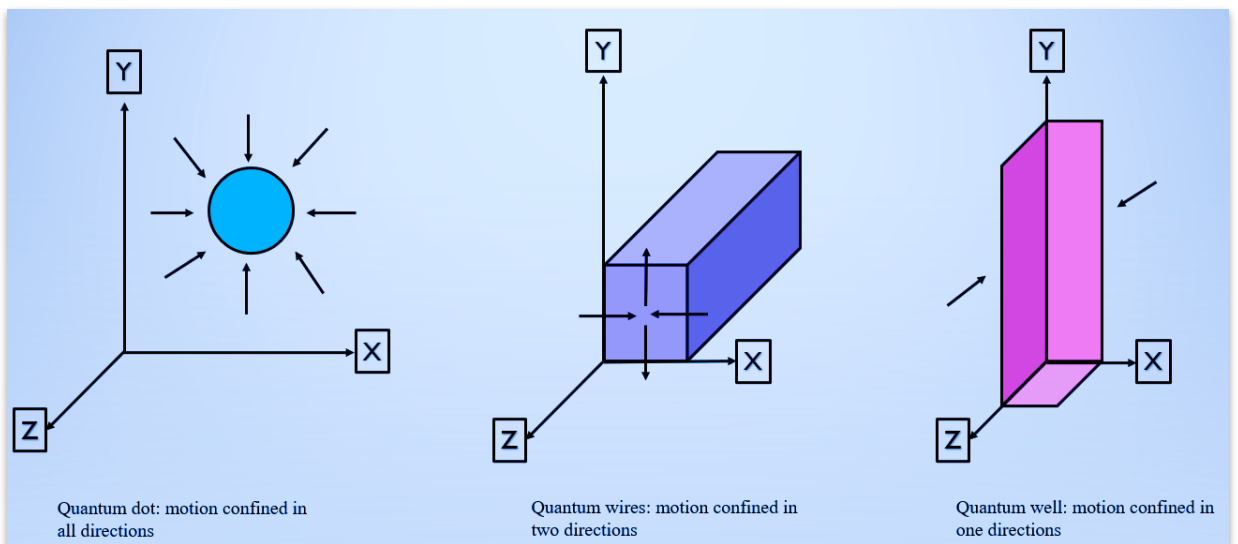Quantum well: motion confined in one directions

Fig.2.4. illustrative representation of quantum confinement in 0D, 1D. and 2D.

2.4 Synthesis of nanoparticles

Synthesis of nanoparticles refers to the process of creating particles at the nanoscale, where at least one of the three dimensions of the particle falls within the nanoscale range (1–100 nm). There are different methods that can be used to synthesise nanoparticles, including physical, chemical, and biological methods. There is also a relatively newer approach known as green synthesis, which offers an alternative to the traditional synthesis methods. Each method has its own principle and procedure for generating nanoparticles.

Some common techniques used in different methods for synthesising nanoparticles include:

- **Chemical Synthesis**: Chemical methods involve chemical reactions and processes to produce nanoparticles. This can include precipitation, sol-gel, hydrothermal synthesis, chemical reduction, and other chemical transformations.
- **Physical Methods**: Physical methods utilize physical processes to create nanoparticles. Examples include physical vapor deposition (PVD), laser ablation, sputtering, and ball milling. These methods typically involve the physical manipulation or fragmentation of bulk materials to obtain nanoparticles.
- **Biological Methods**: Biological synthesis, also known as bio fabrication, involves using biological agents such as bacteria, fungi, or plants to produce nanoparticles. These organisms can either secrete nanoparticles naturally or be engineered to produce specific nanoparticles through their biological processes.
- **Green Synthesis**: Green synthesis methods are focused on the environmentally friendly and sustainable production of nanoparticles. These approaches often utilize natural extracts, biomolecules, or eco-friendly solvents as reducing agents or stabilizers. The use of such green synthesis methods helps minimize the environmental impact and promotes the development of sustainable nanomaterials.

Although there are numerous methods available for nanoparticle synthesis, they can be broadly categorized into two main approaches, which is shown in fig.2.5.
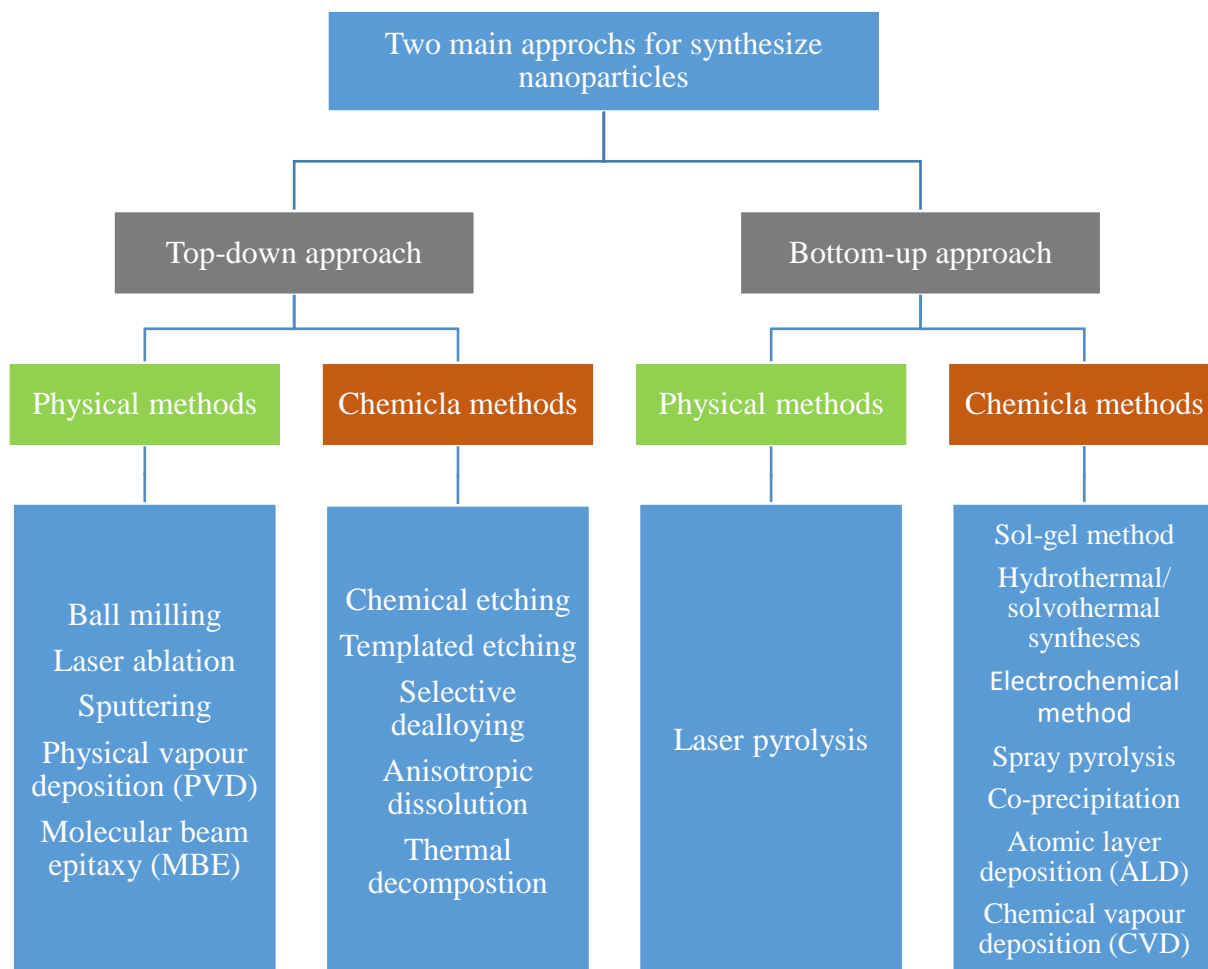
Fig.2.5 physical and chemical methods for top-down and bottom-up synthesis.

2.5 Top-down approach

In the top-down approach, nanoparticle production involves minimizing bulk materials to nanoscale dimensions. There are several physical methods like ball milling, laser ablation, sputtering, etc., and chemical methods that include chemical etching, selective dealloying, thermal depositions, etc. that are used in a top-down approach, but the most common techniques used in a top-down approach involve lithographic patterning techniques that use short-wavelength optical sources. It is used in the fabrication of microelectronics and nanodevices to create patterns and structures on a substrate. It produces nanostructures with high precision and control.

The top-down approach also offers several advantages, like control over the structure, scalability, established techniques, integration with existing technologies, a wide range

of materials, and high resolution and precision. All these advantages make the top-down approach a valuable method for synthesising nanomaterials. However, it's important to consider the limitations and challenges associated with it. There are several imitations of the top-down approach that include limitations in achievable sizes and shapes, material waste, process complexity, surface damage and contamination, difficulty in achieving uniformity, time consumption, and can be very costly. So, it is often necessary to weigh the advantages and disadvantages and consider alternative synthesis methods to overcome limitations or meet specific requirements [11].

2.6 Bottom-up approach

In the bottom-up approach, nanoparticles are synthesized by assembling or growing smaller components such as atoms, molecules, and ions. These components come together to form clusters, which then further aggregate or undergo transformations to eventually form nanoparticles. There are several physical methods, like laser pyrolysis, and some other chemical methods, like the sol-gel method, hydrothermal or solvothermal syntheses, chemical vapour deposition (CVD), etc. Among these sol-gel method is most widely used method because of its simplicity and versatility, and for the large scale production pyrolysis method is most commonly used bottom approach by the industries.

The bottom-up approaches exhibit significant advantages like precise control, uniformity, scalability, versatility, potential for complex structures, integration with other techniques, and reduced energy consumption. These advantages make bottom-up approaches highly valuable in the field of nanotechnology. Although there are several limitations of bottom-up approaches like, limitation control over size and shapes, slow synthesis rates, potential impurities, challenges in upscaling, and may involve the use of expensive precursors or required specialized equipment, which can lead to higher production cost. So, considering the advantages and disadvantages of different synthesis methods is crucial in order to address the limitations and meet specific requirements effectively.

2.7 Application of nanoparticles

Nanoparticles have several uses in a number of various sectors. Because of their distinct characteristics and the ability to improve the performance of materials and systems. Some of the common applications of nanoparticles are:

- **Electronics and Optics**: Nanoparticles are used in various electronic devices such as transistors and memory storage devices, as well as in optoelectronic devices like solar cells and light-emitting diodes (LEDs) [8].

- **Medicine and Healthcare**: Nanoparticles have applications in the medical field, including drug delivery systems, diagnostic imaging, and therapeutics. They can target specific cells or tissues to improve the effectiveness of treatments [9].

- **Environmental Remediation**: Nanoparticles have applications in pollution control and environmental remediation processes, such as water purification and air filtration [10].

- **Energy**: Nanoparticles have applications in the field of energy, including energy storage devices such as batteries and supercapacitors, fuel cells, and catalysts for energy conversion [11, 12].

- **Coatings and Surface Modification**: Nanoparticles are used to enhance the properties of coatings, such as scratch resistance, UV protection, and antimicrobial properties. They are also used for surface modification to improve the performance of materials [13].

- **Catalysis**: Nanoparticles act as catalysts for various chemical reactions, leading to increased reaction rates and selectivity [14].

- **Food and Agriculture**: Nanoparticles have applications in the food industry, where they can be used in packaging to extend shelf life and prevent spoilage. They also have uses in agriculture, such as delivering nutrients to plants and increasing crop yield [15, 16].

- **Textiles and Fabrics**: Nanoparticles can be added to fabrics to enhance their properties, providing benefits such as water repellency, stain resistance, and antimicrobial properties.

- **Environmental Sensing**: Nanoparticles are used in sensors so that they can detect and monitor environmental pollutants, gases, and contaminants [17, 18].

Chapter 3

3.1 Tin Sulfide (SnS)

Tin sulfide (SnS) is a chemical compound composed of tin (Sn) and sulfur (S) atoms. It is a binary-group chalcogenide semiconductor. It has various distinguishing characteristics, including semiconductor nature, direct and indirect bandgap, strong absorption in the UV-Vis light range, layered crystal structure that gives rise to its anisotropic properties, good thermal stability, flexibility in design, earth abundance, and non-toxic. Due to its remarkable characteristic properties, SnS nanoparticles demonstrated great potential in multiple applications which is shown in fig.3.1.
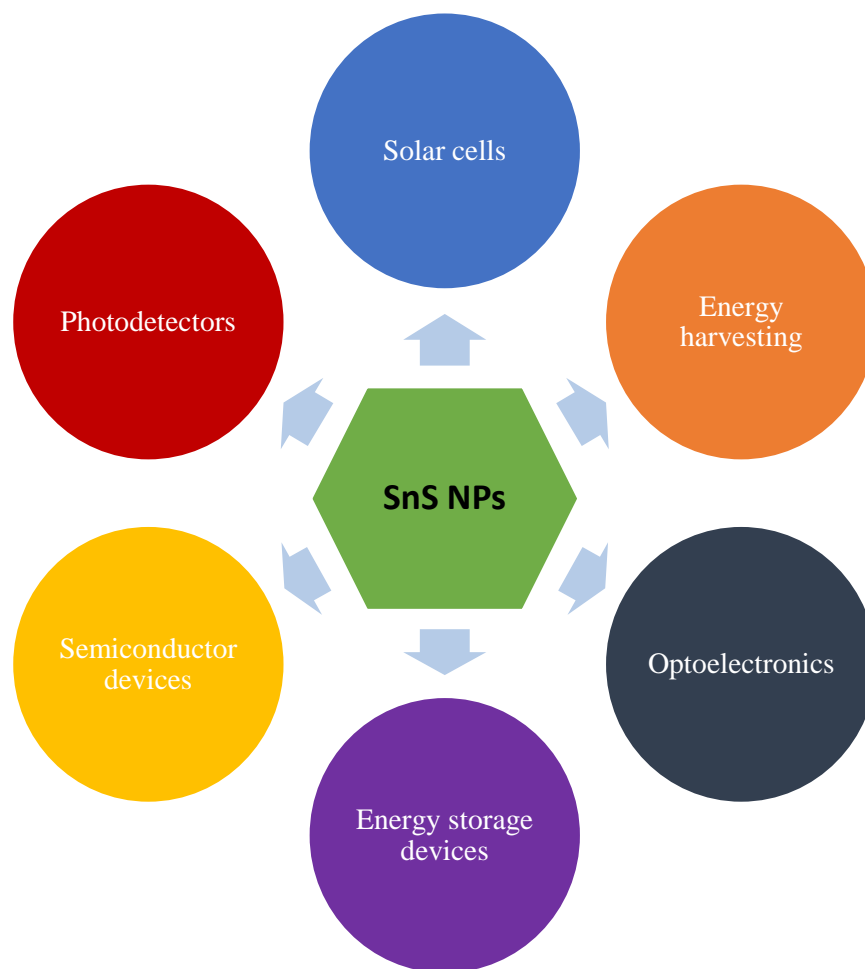
Fig3.1. Applications of SnS nanoparticles.

3.2 Chemical reagents and method used

Tin (II) Chloride ($SnCl_2$), Deionized (DI) water, thiourea (CH_4N_2S), ethylene glycol ($C_2H_6O_2$), citric acid ($C_6H_8O_7$), graphene oxide ($C_{140}H_{42}O_{20}$), N, N-DMF (Dimethylformaide) (C_3H_7NO) and PVDF ($-(C_2H_2F_2)_n-$) powder.

Method used: Hydrothermal synthesis method used to synthesize the SnS NPs. In this method prepared solution is keep into Teflon-lined autoclave and pressure above 1 bar is exerted on it under the high temperature (above 100^0 C).

3.3 Synthesis of SnS nanoparticles

- First, tin (II) chloride was added to Di and stirred for a few minutes.
- Then citric acid was added and stirred for a few minutes.
- Then thiourea was added and stirred for another hour.
- Then the solution was transferred to a Teflon-lined autoclave and put in a hydrothermal, then placed inside an oven for 24 hours at 180 degrees.
- Then it was centrifuged and washed with DI and ethanol several times.
- Then dry for 24 hours at 80 degrees.
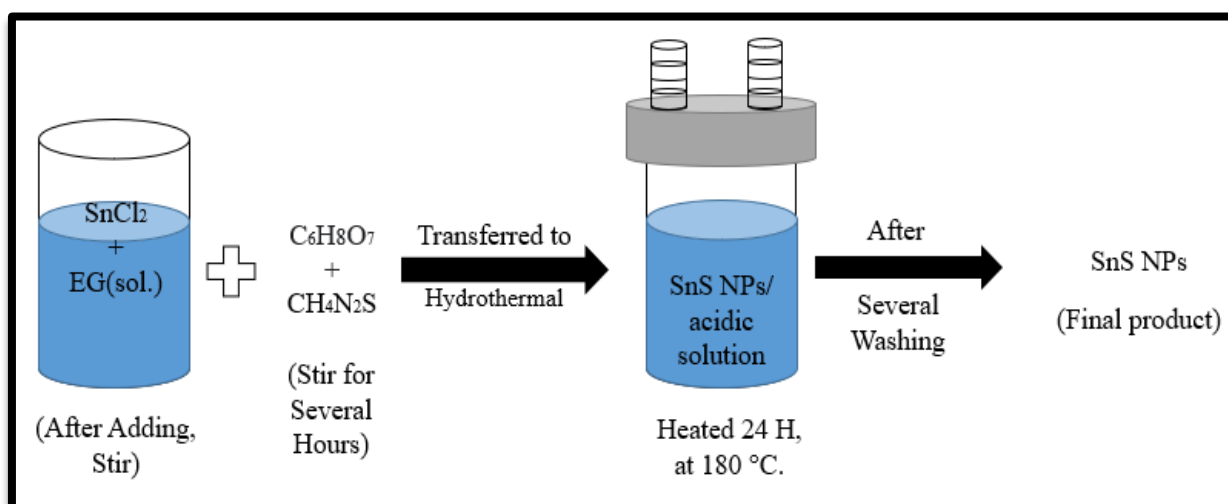- Finally, SnS nanoparticles were obtained.

Fig.3.2. Schematic diagram for the preparation of SnS NPs.

3.4 Synthesis of SnS-rGO nanocomposite

- First, tin (II) chloride was added to EG and stirred for a few minutes.
- Then citric acid and GO were added back-to-back and stirred for a few hours.
- Then thiourea was added, and we continued stirring for 30 minutes.
- Then the solution was transferred to a Teflon-lined autoclave, put in hydrothermal, and placed in an oven for 24 hours at 180 degrees.
- After the solution cooled down to room temperature, it was centrifuged and washed with DI ethanol several times.
- Then dry for 24 hours at 80 degrees.
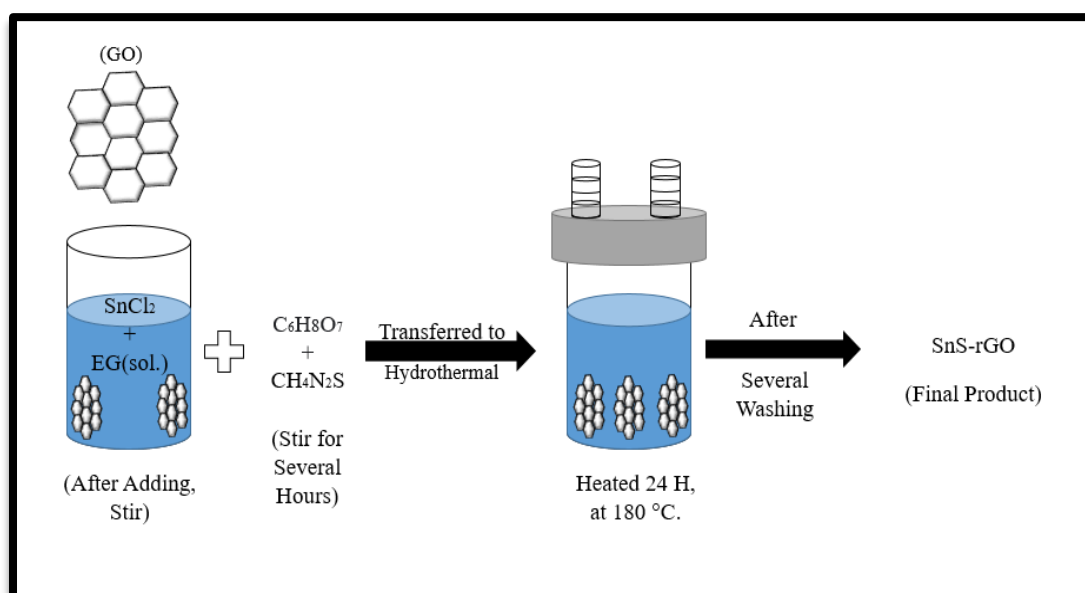- Finally, SnS-rGO nanocomposite was obtained.

Fig.3.3. Schematic diagram for the preparation of SnS/rGO nanocomposite.

3.5 Synthesis of PVDF Thin Films

- First, PVDF powder was added to the DMF solution and stirred for an hour.
- After stirring is complete, keep the solution still for a few minutes.
- Then the solution was drop-cast using a micropipette on glass plates.
- Then dry for 1 hour at 90 degrees.
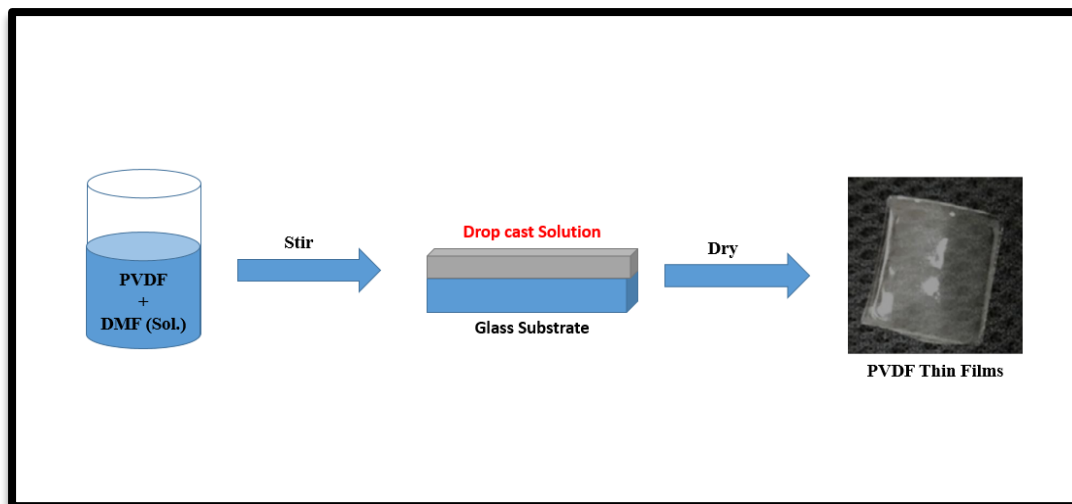- After drying, thin film is removed by sprinkling DI water.

Fig.3.4. Schematic diagram for the preparation of PVDF Thin Film.

3.6 Synthesis of PVDF/SnS-rGO Thin Films

- First, PVDF powder was added to the DMF solution and stirred for a few minutes.
- Then SnS-rGO was added and continued stirring for an hour.
- After stirring is complete, keep the solution still for a few minutes.
- Then the solution was drop-cast using a micropipette on glass plates.
- Then dry for 1 hour at 90 degrees.
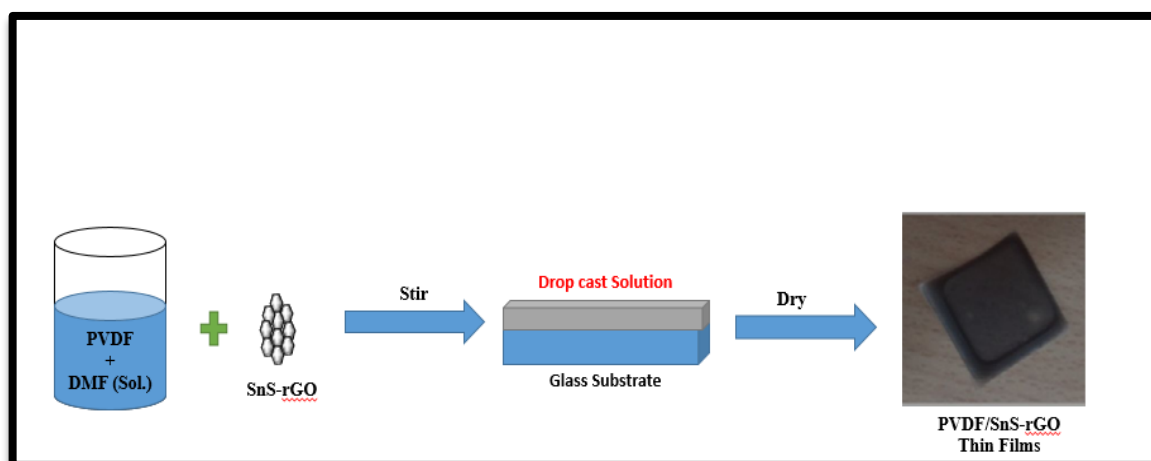- After dying, thin film is removed by sprinkling DI water.

Fig.3.5. Schematic diagram for the preparation of PVDF/ SnS-rGO Thin Film.

3.7 Characterization

The powder X-ray diffraction (XRD) pattern was obtained using CuKα radiation (lambda = 0.154 nm) in the 2-theta range of 20 to 80 degrees on a Bruker D-8 advanced X-ray diffractometer. The optical characteristics have been investigated using UV-visible (UV-vis) and photoluminescence (PL) spectroscopy. The absorption spectra of SnS NPs and SnS-rGO NCS were obtained using the UV-3101PC UV-VIS-NIR spectrophotometer from 200 to 800 nm. A photoluminescence spectrometer (Perkin Elmer, LS 55) with a Xenon lamp as the source and an excitation wavelength of 234 nm was used to measure the PL spectra. ZEISS Gemini field emission scanning electron microscopy (FE-SEM) is used to investigate surface morphology. FTIR spectra in the 400-4000 cm^{-1} wavenumber range were obtained using the Perkin Elmer Spectrum II Fourier transform infrared (FTIR) instrument.

Chapter 4

Results and discussion

4.1 XRD analysis

The XRD diffraction patterns of SnS NPs and SnS-rGO NCs synthesized by the hydrothermal method thiourea as a sulphur source and ethylene glycol as a solvent are shown in Fig. 4.1. The XRD pattern of SnS NPs shows two significant peaks at 2θ: 26.02^0 and 31.9^0, corresponding to planes (120) and (040), respectively, and a few comparatively less intense peaks at 27.9^0 and 51.2^0, corresponding to planes (021) and (151), respectively. All the observed peaks for SnS NPs resemble SnS orthorhombic belonging to space group Pbnm (JCPDS 39-0354). The SnS-rGO XRD pattern exhibits several characteristic SnS peaks at 2θ: 26.6^0, 31.9^0, and 51.4^0, which correspond to planes (120), (040), and (151) respectively, and correlate to SnS orthorhombic belonging to space group Pbnm (JCPDS 39-0354). A shift in peak from 27.90 to 28.30 was observed in the SnS-rGO XRD pattern, this might be caused by the existence of rGO. The shifted peak from 27.9^0 to 28.3^0 corresponds to the hkl plane (111) [19]. Bragg's relation is used to calculate the interplanar spacing (d) of SnS NPs and SnS-rGO NC which is shown in Table 4.1. Bragg's relation:

$$n\lambda = 2\, d\, sin(\theta)$$

Where, n representing the diffraction order, λ is the wavelength of the X-ray beam used in X-ray diffractometer, θ is the angle between the incident beam and the diffracting plane, and d is the interplanar spacing [20].

The average crystallite size for the SnS NPs and SnS-rGO NC is calculated by the Debby Scherrer formula and WH plot, which are shown in Table 4.2. Microstrain calculated using the WH plot is shown in Table 4.2.

Debby Scherrer formula is

$$D = \frac{k\lambda}{\beta \cos\theta}$$

Where D is particle size, K is constant with value 0.94, λ (0.154 nm) is the wavelength used is X-ray diffractometer, β is the full width half maxima (FWHM), and theta (θ) is the Braggs diffraction angle in radian.
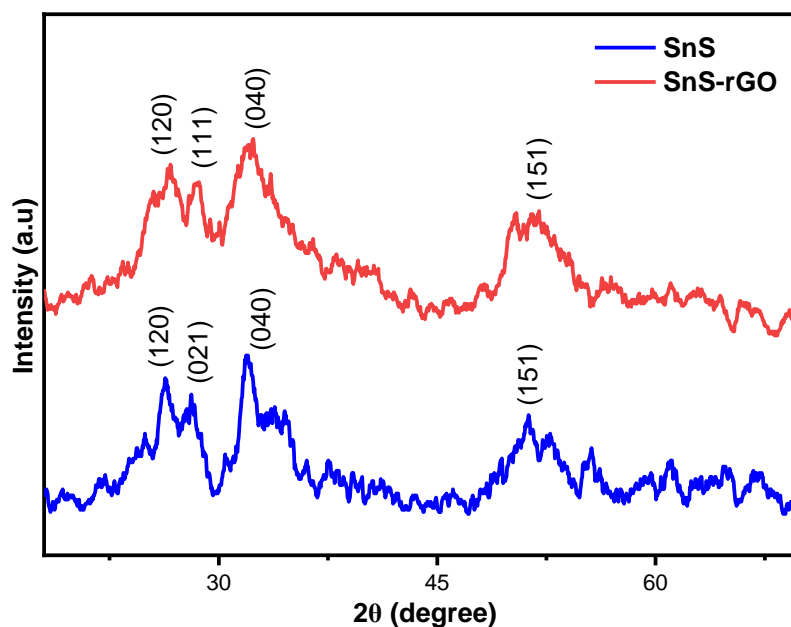

Fig. 4.1. XRD diffraction patterns of SnS NPs and SnS-rGO NCs.

Sample	2θ (degree)	hkl planes	d spacing (nm)
SnS	26.02 27.9 31.9 51.2	(120) (021) (040) (151)	0.34 0.31 0.28 0.17
SnS-rGO	26.6 28.3 31.9 51.4	(120) (021) (040) (151)	0.33 0.31 0.28 0.17

Table 4.2 calculated crystallite size using Scherrer equation and WH plot and strain.

Sample	Average Crystallite size using Scherrer equation	crystallite size from WH Plot	Micro Strain form WH plot
SnS	2.26 nm	2.26 nm	0.00222
SnS-rGO	2.74 nm	9.42 nm	0.03097

Table 4.1 hkl and d spacing value for SnS NPs and SnS-rGO NCs.

4.2 UV-vis analysis

The optical absorption spectra of SnS NPs and SnS-rGO NCs in the wavelength range of 200nm to 800nm were analyzed using the UV-3101PC UV-VIS-NIR spectrophotometer, as shown in Fig. 4.2. In the case of SnS NPs, the absorption spectra of SnS NPs demonstrate four absorption peaks. The first three peaks were identified in the UV region at 220, 330, and 390 nm, whereas the fourth occurs in the UV-vis region as a broad band from 550 to 800 nm. In case of SnS-rGO NCs four absorption peaks are observed. First three peaks lie in the UV region at 22a0, 264, and 340 nm. While the fourth one is observed as abroad band from 390 to 800 nm [28]. So, we can say SnS, SnS-rGO are capable of absorbing light of shorter or longer wavelengths. In the case of SnS-rGO NCs, four absorption peaks have been detected. The initially identified three peaks, at 220, 264, and 340 nm, were in the ultraviolet region. The fourth one has been observed as a broad band from 390 to 800 nm [21]. After observing the absorption spectra of SnS NPs and SnS-rGO NCs, we can conclude that SnS NPs and SnS-rGO NCs are capable of absorbing light with shorter or longer wavelengths. Further, we have drawn the Tauc plot to calculate the direct and indirect band gap for SnS NPs and SnS-rGO NCs. which is shown in Fig. 4.3. and Table 4.3.

tauc's equation:

$$(\alpha h v)^r = \beta(h v - E_g)$$

where β is constant, α is the absorption constant, h is the plank constant, v is the photon's frequency, E_g is the energy bandgap, and r depends on the electronic transition. The value of r is 1/2 and 2 for indirect and direct transition respectively [22].
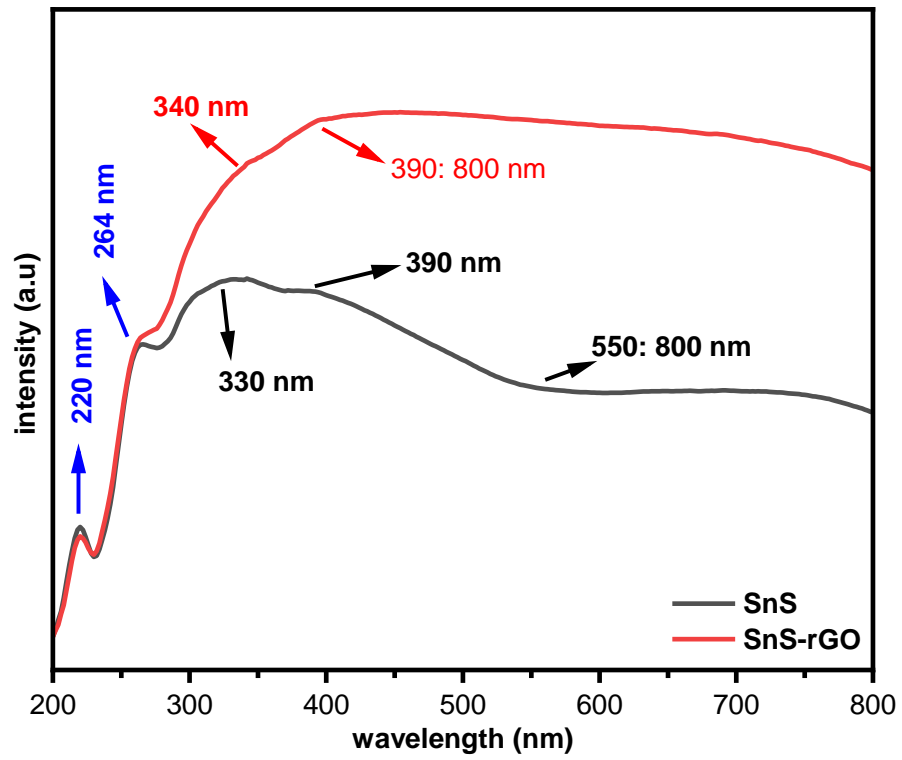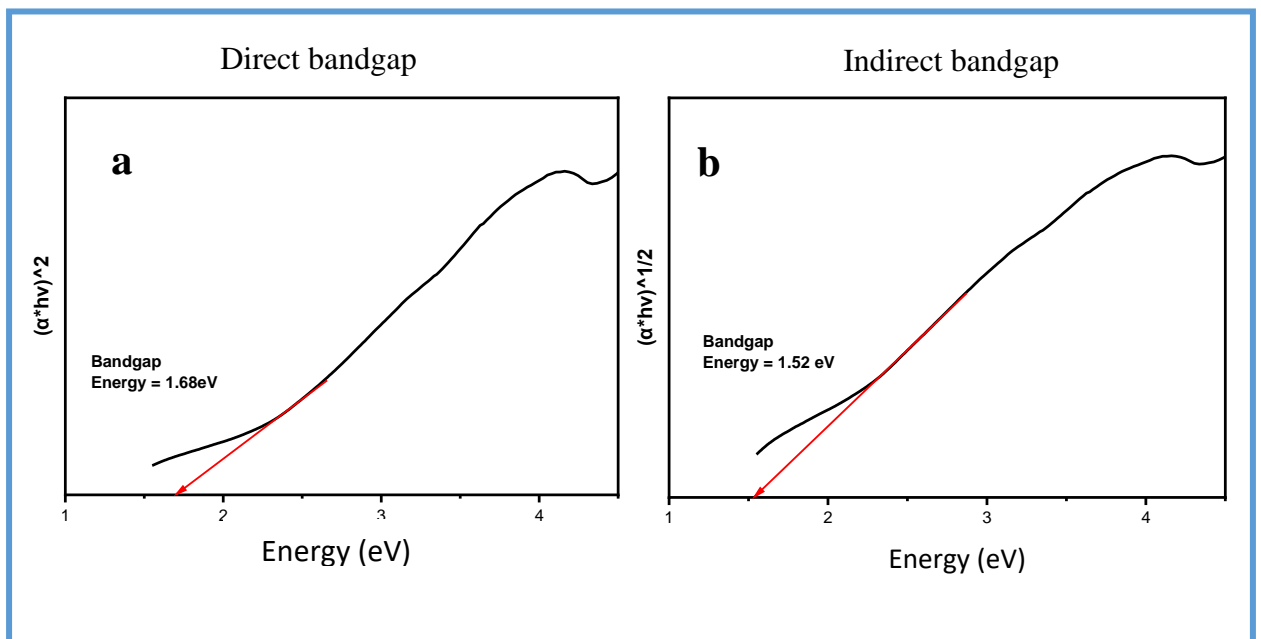
Fig 4.2 UV-vis Spectra of SnS NPs and SnS-rGO NCs.

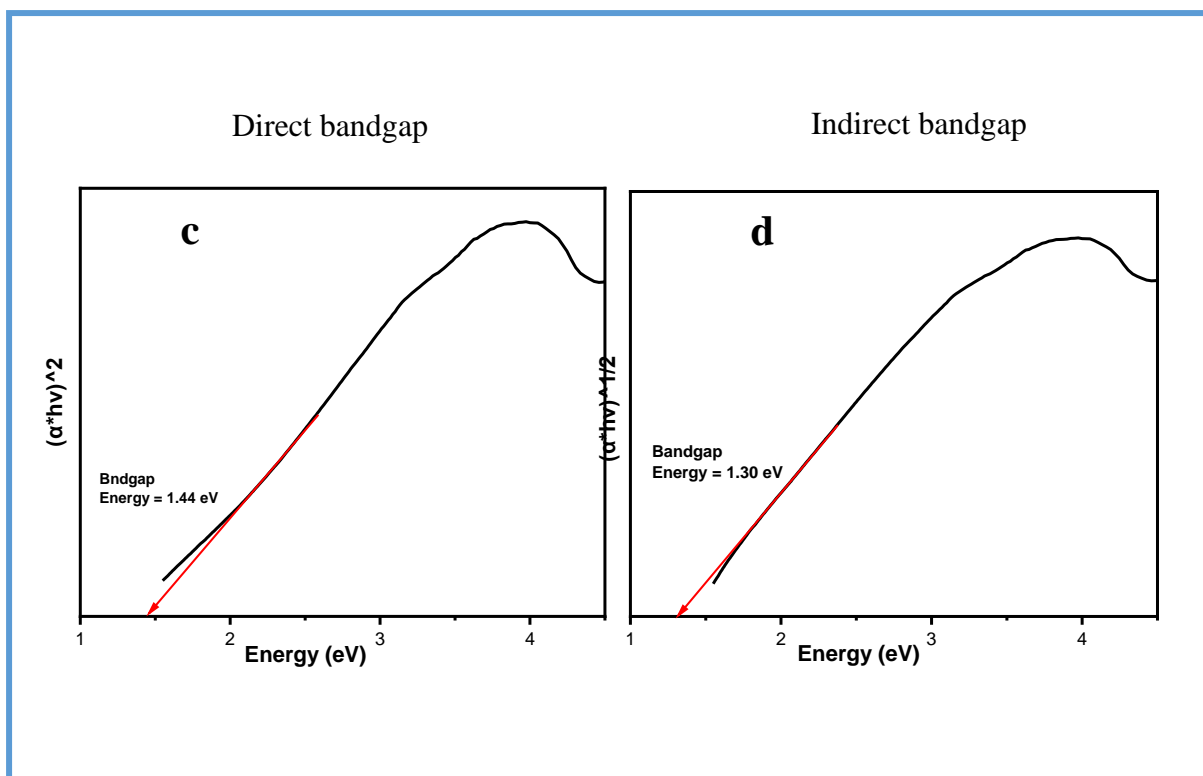Fig. 4.3 (a,b) Direct and indirect bandgap of SnS NPs

Fig. 4.3. (c, d) Direct and indirect bandgap of SnS-rGO NCs.

Sample	Direct bandgap (eV)	Indirect bandgap (eV)
SnS	1.68	1.52
SnS-rGO	1.44	1.30

Table 4.3 direct and indirect bandgap values of SnS NPs and SnS-rGO NCs.

4.3 Photoluminescence (PL) analysis

The FP-8300 spectrofluorometer was used to measure the PL intensity of SnS NPs and SnS-rGO NCs in the wavelength range of 200 to 800 nm, with an excitation wavelength of 242 nm. The PL spectra of SnS NPs and SnS-rGO NCs are shown in Fig. 4.4. The PL spectra of SnS NPs and SnS-rGO NCs show identical emission peaks, as can be observed in Fig. 4.4. The first prominent emission peak was spotted at 390 nm in the near UV-vis region, while the other two less intense emission peaks were observed at 467 and 481 nm in the UV-vis region.
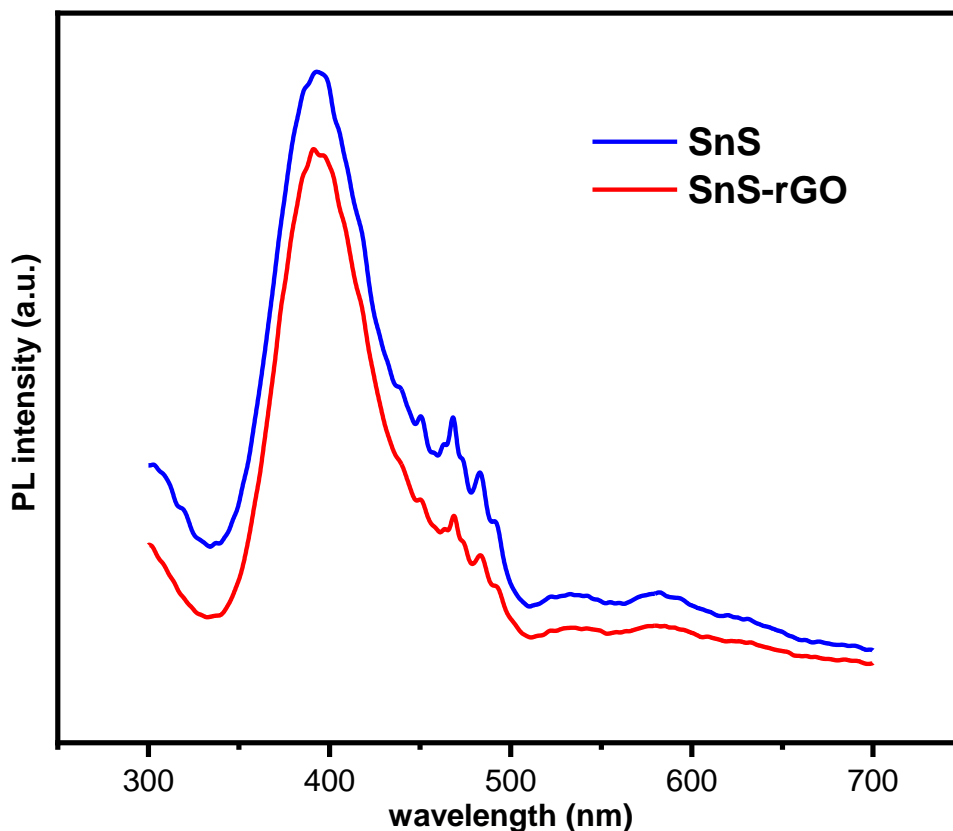
Fig. 4.4 PL spectra of SnS NPs and SnS-rGO NCs.

4.4 Fourier transform infrared (FTIR) analysis

The Perkin Elmer Spectrum II Fourier transform infrared (FTIR) spectrometer was used to obtain SnS NPs and SnS-rGO NCs FTIR spectra in the range of 400-4000 cm-1 wavenumber. Fig. 4.5 (a, b) shows the FTIR spectra of SnS NPs and SnS-rGO NCs. In the case of SnS NPs, a significant vibrational peak at 540 cm^{-1} is observed, indicating the presence of an Sn-S bond [23]. Some other minor peaks have been seen at 1337 and 1625 cm^{-1}, which could be attributed to S-OH and H_2O modes. Sn-S features can be attributed to the peak between 1000 and 1200 cm^{-1} [24]. In the case of SnS-rGO NCs, one strong and one minor peak appear at 540 cm^{-1}, and 620 cm^{-1} is attributable to the Sn-S bond. Other peaks at 877 cm^{-1}, 1040 cm^{-1}, 1184 cm^{-1}, 1425 cm^{-1}, 1693 cm^{-1}, and 2890–3000 cm^{-1} can be ascribed to C-H bending, S=O stretching, C-O stretching, O-H bending, Sn-OH, H_2O mode, and the OH stretching vibration.
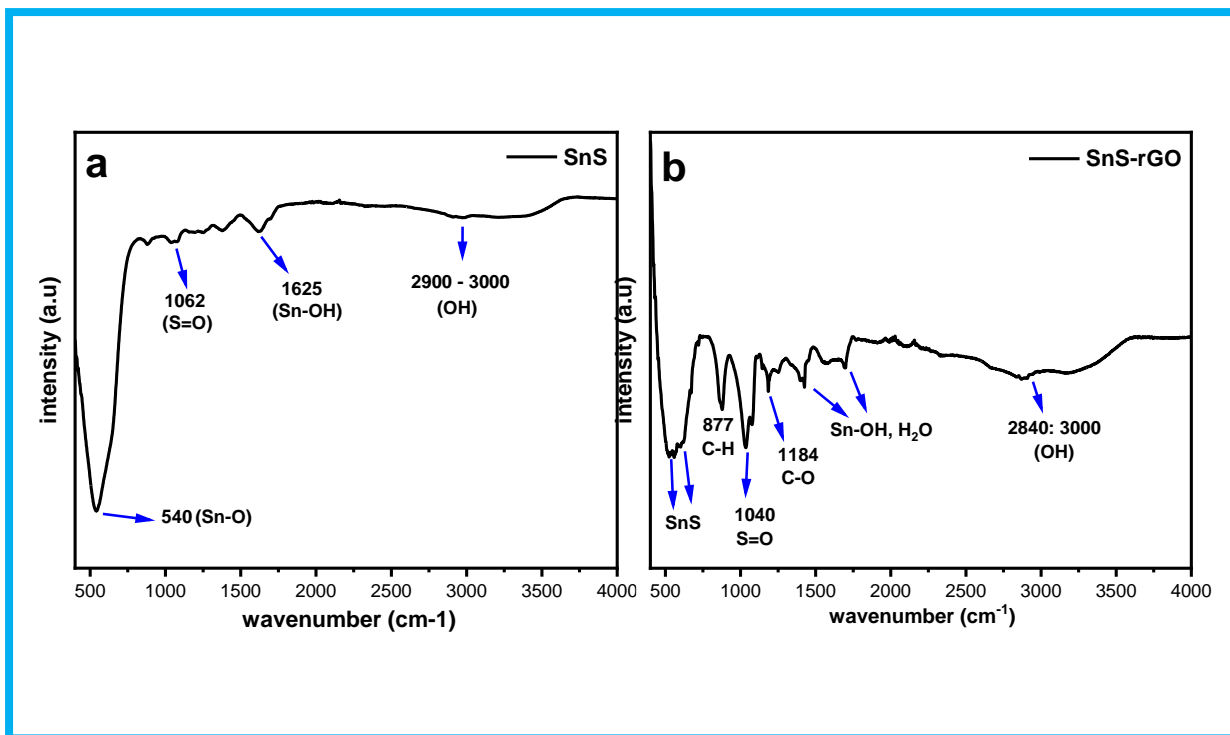
Fig. 4.5. (a) FTIR spectra of SnS NPs, (b) FTIR spectra of SnS-rGO NCs.

4.5 FE-SEM and EDX analysis

The ZEISS Gemini field emission scanning electron microscopy (FE-SEM) is used to analyse the shape and structure of SnS NPs and SNS-rGO NCs. The EDX pattern reveals the elemental composition of the SnS NPs and SnS-rGO NCs. Figures (4.6) and (4.7) show FE-SEM and EDX images of SnS NPs and SnS-rGO NCs, respectively. In the case of SnS NPs (fig. 4.6), agglomerated small-size spherical particle formation is observed at various resolutions. The presence of Sn and S elements is verified by the EDX pattern of SnS NPs, with atomic percentages of 53.81% and 46.13%, respectively. In the case of SnS NCs (fig. 4.7), transfomation in morphology and the formation of rGO petals are observed, which might be attributable to rGO doping in SnS. From Fig. 4.7, aggregated SnS NPs can be observed on the surface of rGO petals. The EDX pattern of SnS-rGO NCs verifies the presence of Sn, S, O, and C elements with atomic percentages of 15.95%, 23.10%, 12.48%, and 48.47%, respectively.
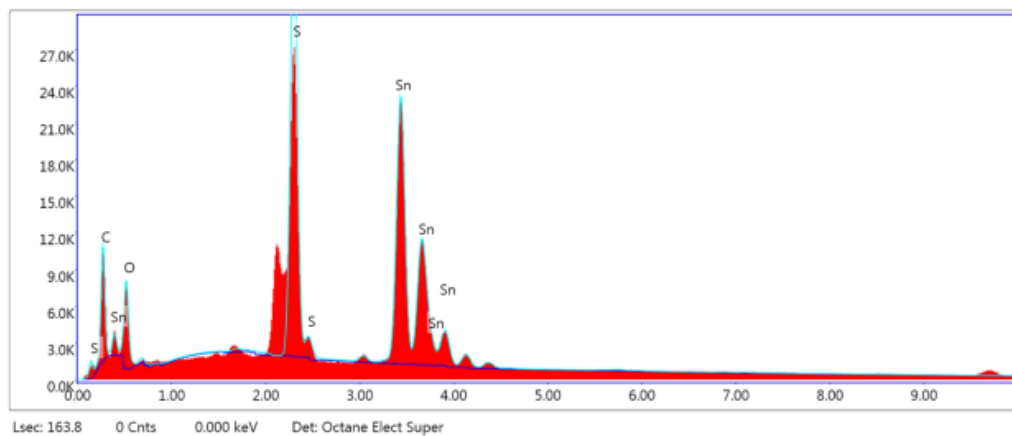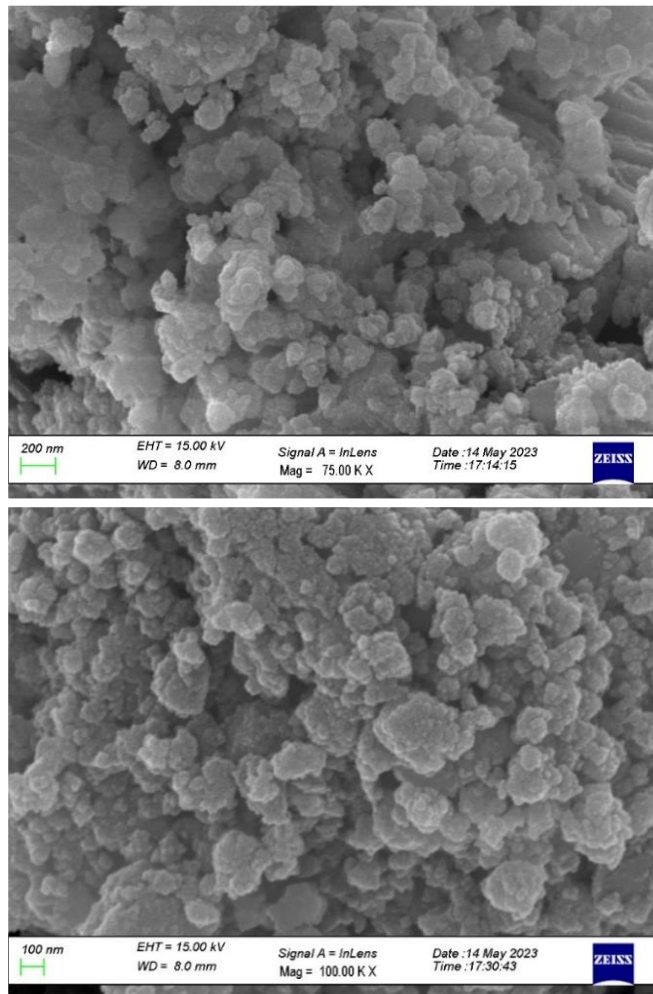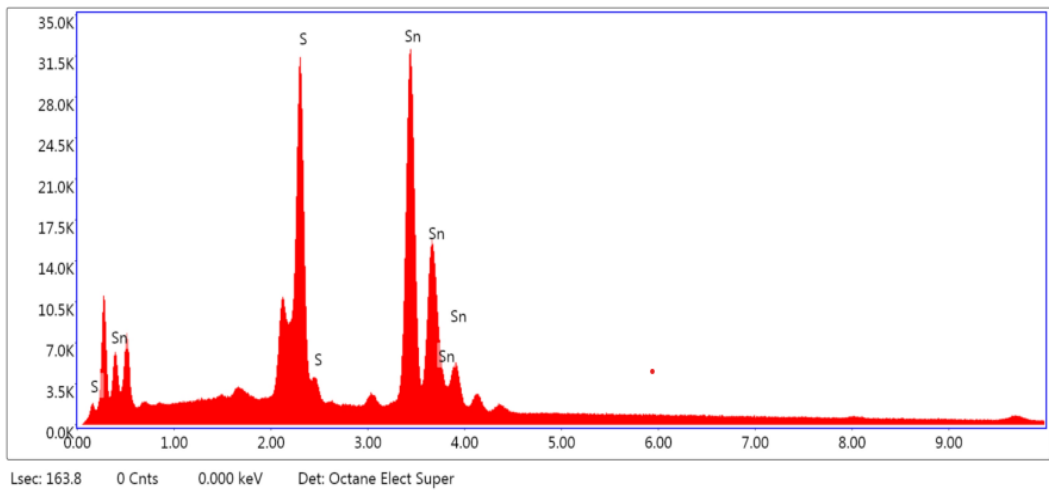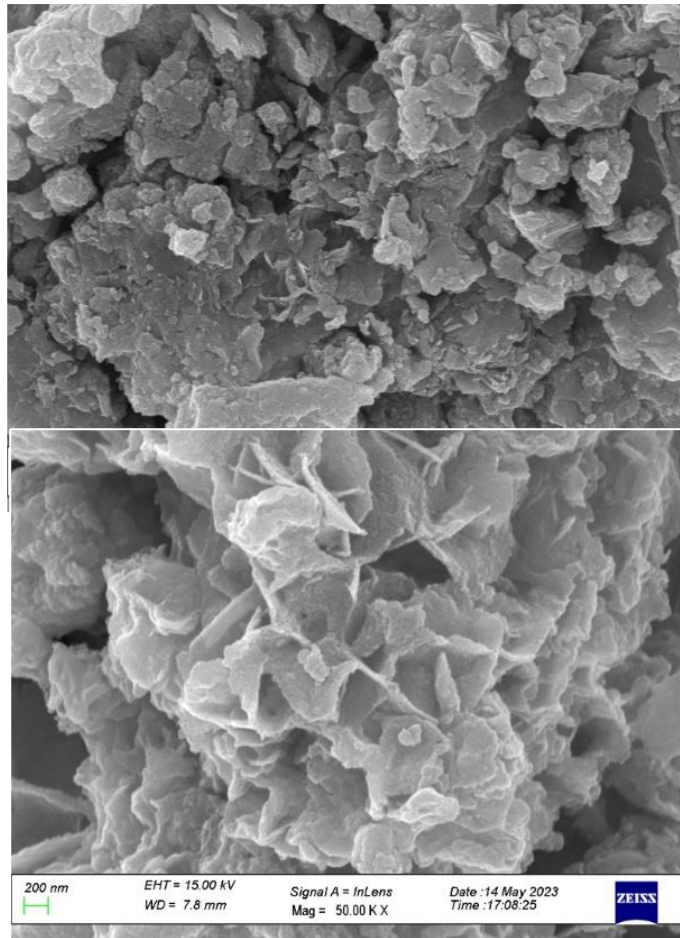
eZAF Smart Quant Results

Element	Weight %	Atomic %	Net Int.	Error %	Kratio	Z	A	F
C K	17.04	48.47	290.40	9.72	0.0496	1.3206	0.2203	1.0000
O K	5.84	12.48	226.90	9.64	0.0190	1.2647	0.2575	1.0000
S K	21.68	23.10	2013.30	3.15	0.2134	1.1311	0.8541	1.0189
SnL	55.43	15.95	1477.30	1.92	0.4524	0.8106	1.0076	0.9993

Fig. 4.6 FESEM and EDX images of SnS NPs.

Element	Weight %	Atomic %	Net Int.	Error %	Kratio	Z	A	F
S K	23.94	53.81	2193.70	3.65	0.2500	1.2721	0.8043	1.0207
SnL	76.06	46.19	2059.70	2.03	0.6781	0.9145	0.9754	0.9994

Fig. 4.7 FESEM and EDX images of SnS-rGO NCs.

Chapter 5

5.1 <u>Conclusion</u>

This thesis explores the fascinating world of nanomaterials, which have been used since ancient times for various purposes. We trace the evolution of nanomaterials and how they gave rise to new fields of study and applications. We also examine the questions that drive the research and innovation in nanomaterials: What are their properties and application. How can we create them. And after thoroughly investigating and assessing various methods of synthesis. we used the hydrothermal technique to effectively synthesize SnS NPs and SnS-rGO NCs. The crystallite size of the particle was calculated using the Deby-Sherer equation., and Bragg's relation was utilized to determine the interplanar d-spacing. Tauc's approach is used for calculating the direct and indirect bandgaps. The synthesized SnS NPs and SnS-rGO NCs exhibit UV and UV-vis absorption and emission peaks, making them viable candidates for solar cell, energy harvesting and optoelectronic characteristics. The FE-SEM analysis indicates that SnS NPs are effectively connected to the rGO surface in the SnS-rGO NCs, which may lead to improved catalytic and other capabilities. Furthermore, the synthesized SnS NPs and SnS-rGO NCs also have potential in various applications, such as energy storage devices and gas sensing. So, in the future, we would like to explore these materials for energy harvesting application.

Reference:

1. Junk, A., & Riess, F. (2006). From an idea to a vision: There's plenty of room at the bottom. *American Journal of Physics*, *74*(9), 825–830. https://doi.org/10.1119/1.2213634

2. Tersoff, J., & Hamann, D. R. (1985). Theory of the scanning tunneling microscope. *Physical Review*, *31*(2), 805–813. https://doi.org/10.1103/physrevb.31.805

3. Aldersey-Williams, H. (1996). The most beautiful molecule: the discovery of the buckyball. *Choice Reviews Online*, *33*(09), 33–5108. https://doi.org/10.5860/choice.33-5108

4. Ananthaiah, R. (1997). Discovery of Fullerenes. *Resonance*, *2*(1), 68–73. https://doi.org/10.1007/bf02838784

5. Iijima, S. (1991b). Helical microtubules of graphitic carbon. *Nature*, *354*(6348), 56–58. https://doi.org/10.1038/354056a0

6. Ramalingam, G., Kathirgamanathan, P., Ravi, G., Elangovan, T., Kumar, B. A., Manivannan, N., & Kasinathan, K. (2020). Quantum Confinement Effect of 2D Nanomaterials. In *IntechOpen eBooks*. https://doi.org/10.5772/intechopen.90140

7. Abid, N., Khan, A. M., Shujait, S., Chaudhary, K., Ikram, M., Imran, M., Haider, J., Maaz, K., Khan, Q., & Maqbool, M. (2021). Synthesis of nanomaterials using various top-down and bottom-up approaches, influencing factors, advantages, and disadvantages: A review. *Advances in Colloid and Interface Science*, *300*, 102597. https://doi.org/10.1016/j.cis.2021.102597

8. Mascher, P. (2015). Nanoparticles in dielectric matrix for electronics and optics: from the fabrication to the devices. *Physica Status Solidi*. https://doi.org/10.1002/pssc.201570107

9. Zhang, L., Gu, F., Chan, J. C., Wang, S. A., Langer, R., & Farokhzad, O. C. (2008). Nanoparticles in Medicine: Therapeutic Applications and Developments. *Clinical Pharmacology & Therapeutics*, *83*(5), 761–769. https://doi.org/10.1038/sj.clpt.6100400

10. Das, P. K., Mohanty, C., Purohit, G., Mishra, S., & Palo, S. (2022). Nanoparticle assisted environmental remediation: Applications, toxicological implications and recommendations for a sustainable environment. *16. Nanoparticle Assisted Environmental Remediation: Applications, Toxicological Implications and Recommendations for a Sustainable Environment*, *18*, 100679. https://doi.org/10.1016/j.enmm.2022.100679

11. 17 (11) Pomerantseva, E., Prato, M., Feng, X., Cui, Y., & Gogotsi, Y. (2019). Energy storage: The future enabled by nanomaterials. *Science*, *366*(6468). https://doi.org/10.1126/science.aan8285

12. López, M., & Ustarroz, J. (2021). Electrodeposition of nanostructured catalysts for electrochemical energy conversion: Current trends and innovative strategies. *Current Opinion in Electrochemistry*, *27*, 100688. https://doi.org/10.1016/j.coelec.2021.100688

13. Vidales-Herrera, J., & López, I. (2020). Nanomaterials in coatings: an industrial point of view. In *Elsevier eBooks* (pp. 51–77). https://doi.org/10.1016/b978-0-12-821381-0.00003-x

14. Astruc, D. (2020). Introduction: Nanoparticles in Catalysis. *Chemical Reviews*, *120*(2), 461–463. https://doi.org/10.1021/acs.chemrev.8b00696

15. Kaningini, G. A., Nelwamondo, A. M., Azizi, S., Maaza, M., & Mohale, K. C. (2022). Metal Nanoparticles in Agriculture: A Review of Possible Use. *Coatings*, *12*(10), 1586. https://doi.org/10.3390/coatings12101586

16. Kashyap, P. L., Xiang, X., & Heiden, P. A. (2015). Chitosan nanoparticle based delivery systems for sustainable agriculture. *International Journal of Biological Macromolecules*, *77*, 36–51. https://doi.org/10.1016/j.ijbiomac.2015.02.039

17. Rassaei, L., Marken, F., Sillanpää, M., Amiri, M., Cirtiu, C. M., & Sillanpää, M. (2011). Nanoparticles in electrochemical sensors for environmental monitoring. *Trends in Analytical Chemistry*, *30*(11), 1704–1715. https://doi.org/10.1016/j.trac.2011.05.009

18. Willner, M. R., & Vikesland, P. J. (2018). Nanomaterial enabled sensors for environmental contaminants. *Journal of Nanobiotechnology*, *16*(1). https://doi.org/10.1186/s12951-018-0419-1

19. Mani, P., Manikandan, K., & Prince, J. J. (2016). Influence of molar concentration on triethanolamine (TEA) added tin sulfide (SnS) thin films by

SILAR method. *Journal of Materials Science: Materials in Electronics*, *27*(9), 9255–9264. https://doi.org/10.1007/s10854-016-4963-x

20. Zaaba, N. I., Foo, K. L., Hashim, U., Tan, S. M., Liu, W., & Voon, C. H. (2017). Synthesis of Graphene Oxide using Modified Hummers Method: Solvent Influence. *Procedia Engineering*, *184*, 469–477. https://doi.org/10.1016/j.proeng.2017.04.118

21. Mostafa, A. M., Mwafy, E. A., & Hasanin, M. (2020). One-pot synthesis of nanostructured CdS, CuS, and SnS by pulsed laser ablation in liquid environment and their antimicrobial activity. *Optics and Laser Technology*, *121*, 105824. https://doi.org/10.1016/j.optlastec.2019.105824

22. Makuła, P., Pacia, M. Z., & Macyk, W. (2018). How To Correctly Determine the Band Gap Energy of Modified Semiconductor Photocatalysts Based on UV–Vis Spectra. *Journal of Physical Chemistry Letters*, *9*(23), 6814–6817. https://doi.org/10.1021/acs.jpclett.8b02892

23. Meyer, E. L., Mbese, J. Z., Agoro, M. A., & Taziwa, R. (2020). Optical and structural-chemistry of SnS nanocrystals prepared by thermal decomposition of bis(N-di-isopropyl-N-octyl dithiocarbamato)tin(II) complex for promising materials in solar cell applications. *Optical and Quantum Electronics*, *52*(2). https://doi.org/10.1007/s11082-020-2212-2

24. Henry, J., Mohanraj, K., Kannan, S., Barathan, S., & Sivakumar, G. (2013). Effect of selenium doping on structural and optical properties of SnS:Se thin films by electron beam evaporation method. *European Physical Journal-applied Physics*, *61*(1), 10301. https://doi.org/10.1051/epjap/2012120359

Appendix 1: Plagiarism report